Determination of the atomic density of rubidium-87*

Zhao Meng(赵 盟), Zhang Kai(张 凯), and Chen Li-Qing(陈丽清)†

State Key Laboratory of Precision Spectroscopy, Department of Physics, East China Normal University, Shanghai 200062, *China*

(Received 12 February 2015; revised manuscript received 15 April 2015; published online 21 July 2015)

Atomic density is a basic and important parameter in quantum optics, nonlinear optics, and precision measurement. In the past few decades, several methods have been used to measure atomic density, such as thermionic effect, optical absorption, and resonance fluorescence. The main error of these experiments stemmed from depopulation of the energy level, self-absorption, and the broad bandwidth of the laser. Here we demonstrate the atomic density of ^{87}Rb vapor in paraffin coated cell between 297 K and 334 K mainly using fluorescence measurement. Optical pumping, anti-relaxation coating, and absorption compensation approaches are used to decrease measurement error. These measurement methods are suitable for vapor temperature at dozens of degrees. The fitting function for the experimental data of ^{87}Rb atomic density is given.

Keywords: atomic density, ^{87}Rb vapor, fluorescence, absorption compensation

PACS: 42.50.Gy, 42.30.Kq **DOI:** 10.1088/1674-1056/24/9/094206

1. Introduction

In the last two decades, due to the rapid development of quantum information and precision measurement,[1] many phenomena of quantum optics and nonlinear optics[2,3] in the alkali atomic ensemble[4–7] have been brought into focus. The atomic density of the atomic ensemble is important for some phenomena in quantum optics and for the precision of the parameters in a precision measurement; for example, super-radiance,[8] magnetic measurement,[9,10] and atomic clock.[11,12] There are mainly two kinds of atomic ensembles. One is the cold atomic ensemble, which is often used in quantum information,[13] but its density number is difficult to improve. The other is the atomic vapor, which is more often used in precision measurement.[1] Many theoretical and experimental approaches have been tried to obtain accurate data of atomic density. Killian[14] measured the vapor pressure of natural rubidium and potassium by thermionic effect between 312 K and 377 K in 1926. Gallagher and Lewist[15] measured the vapor pressure of rubidium-85 by optical absorption at temperatures from 330 K to 370 K in 1973. Fairbank *et al.*[16] measured the density of sodium vapor at low temperature using resonance fluorescence measurement in 1974. In 1988, van der Spek *et al.*[17] measured the vapor pressure of natural rubidium between 250 K and 298 K by combined fluorescence and absorption measurements. In these experiments, the main error stemmed from depopulation of the energy level, self-absorption, and broad bandwidth of the laser. In 2013, Tehranchi *et al.*[18] measured the atomic number density of Rb vapor between 470 K and 550 K using spectral Faraday Rotation measurement, which is more suitable to measure the density at high temperature.

Natural rubidium is a mixture of two isotopes. The ^{85}Rb constitutes 72%, and the remaining 28% is ^{87}Rb. The pure ^{87}Rb atomic vapor is one of the most popular ensembles in quantum information and precision measurement,[1] but until now there are not any experimental reports on its density or vapor pressure. In this paper, we will demonstrate the atomic density of pure ^{87}Rb vapor in the temperature range from 297 K to 334 K, which is often used in experiments.[19] We combine fluorescence measurement, optical pumping, paraffin coating, absorb compensation, and single-photon detection system to reduce the inaccuracy resulting from the self-absorption and depopulation effects. In addition, the laser of 300 kHz narrow bandwidth is used in experiment to avoid the error from the broad-bandwidth laser.

2. Experimental setup

The energy levels of ^{87}Rb atom and time sequence are given in Figs. 1(a) and 1(b) together with laser frequencies. The two higher energy states $|e_1\rangle$ and $|e_2\rangle$ are the excited states $|5^2P_{1/2}, F = 2\rangle$ and $|5^2P_{3/2}, F = 3\rangle$. The two lower energy states $|g\rangle$ and $|m\rangle$ are the hyperfine split ground states $|5^2S_{1/2}, F = 1, 2\rangle$ with a frequency difference of 6.87 GHz. In our experiment, the atomic density of the pure ^{87}Rb atom is measured mainly using fluorescence method with a narrow-bandwidth laser L. Under the nature state, the atoms populate at $|g\rangle$ and $|m\rangle$ levels equally. As shown in Fig. 1(b), before the laser pulse L, an optical pumping (OP) pulse which is resonant with the transition from $|m\rangle$ to $|e_2\rangle$, interacts with the atoms to prepare most atoms on $|g\rangle$ state to reduce the absorption of the subsequent fluorescence. After OP pulse, a laser pulse L with width of 100 ns enters the atoms to generate the fluorescence F.

*Project supported by the Natural Science Foundation of China (Grant Nos. 11274118 and 11474095), the Innovation Program of Shanghai Municipal Education Commission of China (Grant No. 13ZZ036), and the Fundamental Research Funds for the Central Universities of China.

†Corresponding author. E-mail: lqchen@phy.ecnu.edu.cn

© 2015 Chinese Physical Society and IOP Publishing Ltd

The F consists of two kinds of fluorescences F_g and F_m, corresponding to the transitions $|e_1\rangle \rightarrow |g\rangle$ and $|e_1\rangle \rightarrow |m\rangle$, respectively. The laser L is resonant on the transition of $|g\rangle \rightarrow |e_1\rangle$.

The experimental setup is sketched in Fig. 1(c), the paraffin-coated cylindrical Pyrex cell C (50 mm in length, 20 mm in diameter) is filled with ^{87}Rb vapor. The cell is placed inside a four-layer magnetic shield to reduce stray magnetic fields. The cell temperature is limited to below 343 K because of the melting point of paraffin coating. The temperature of the C cell is controlled by using a bifilar resistive heater outside the shield and temperature controller. The precision of temperature controller is 0.1 K, which is enough for our experiment because the atomic density is measured every 1.0 K. The OP and L lasers both come from two independent external cavity diode lasers. The bandwidth of the laser L is 300 kHz, which is much smaller than the Doppler width 0.5–1.0 GHz. The intensity of OP laser is 240 mW. The intensity of the laser L is about 20 μW and the diameter is 1.5 mm in the cell C. The intensity of the fluorescence, which is at single photon level, is very low compared with those of OP and L pulses, so some optical filters including polarization filter, spatial filter, and frequency filter, are required. Firstly, the fluorescence photons with random polarization and pulse L with vertical polarization pass through a polarized beam splitter (PBS) together to filter most L photons for polarization filtering. Then, the F and leaking L photons are collected into a single-mode fiber at 2 degree angle for spatially filtering, and are at last sent into an etalon (bandwidth of 12 MHz and fineness of 800) to filter the leaking L photons 29 dB further. The transmission rate of the fluorescence photons is 80%. The frequency of F_g is the same as that of the L photons, so finally only F_m photons can transmit through the etalon. The F_m photons are detected and analyzed by a single-photon detector D_1 (PerkinElmer, SPCM-AQRH-14-FC) and single channel analyzer. In experiments, in order to obtain high population rates of the $|g\rangle$ state along the light paths of the laser L and F photons at 2 degree angle to reduce the absorption of F_m, the OP pulse is split into two parts, OP_1 and OP_F, overlapping with L and F. The powers of OP_1 and OP_F pulses are both equal to 120 ± 0.2 mW. The population rates of the $|m\rangle$ state along two light paths are about 1%–3% at different temperatures. All of the experimental conditions are fixed when the temperature of the cell is changed.

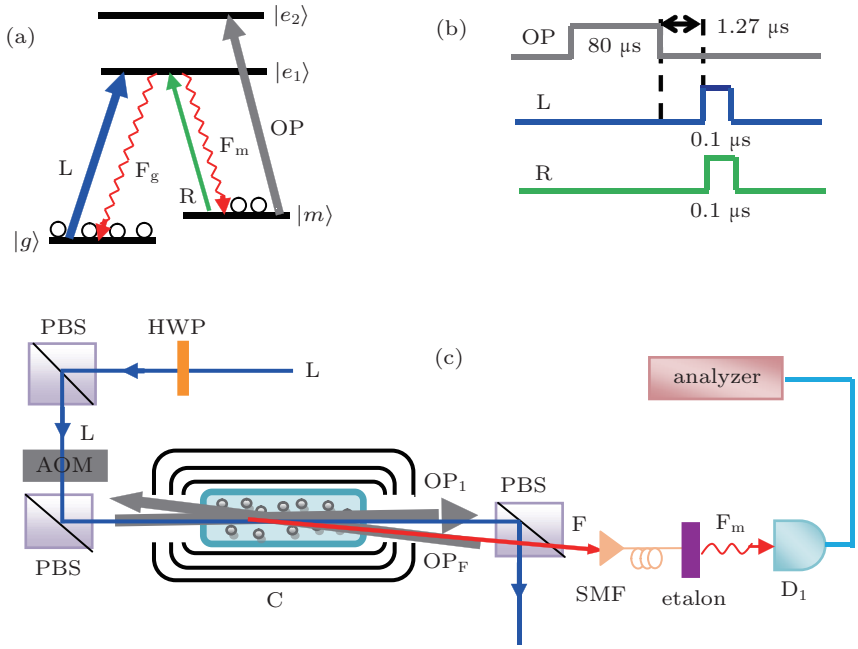


Fig. 1. (color online) (a) Energy levels of ^{87}Rb atom. (b) Time sequence. (c) Experimental layout. C: the pure ^{87}Rb atomic vapor; PBS: polarized beam splitter; HWP: half wave plate; D_1: single photon detector; SMF: single mode fiber; AOM: acousto-optical modulator; F: fluorescence; OP_1 and OP_F: optical pumping lasers.

3. Results

Figure 2 shows the main results of our experiment. The x axis shows the temperature of the cell and the y axis shows the detected intensity of the fluorescence F_m. The intensity of the fluorescence increases monotonically with the temperature from 297 K to 325 K, and then decreases when the temperature continues to increase. This is mainly due to the absorption by $|m\rangle$ atoms. In experiment, we can pump most, but not all, atoms on the $|g\rangle$ energy level by optical pumping, and the rest atoms still populated at the $|m\rangle$ state will absorb the generated fluorescence F_m. The absorption rate has a linear relation with the number of atoms, which increases with temperature, so the absorption rate increases with the cell temperature, especially at higher temperature. From Fig. 2, it is obvious that the absorption by $|m\rangle$ atoms has a large effect on the measurement of the atomic density when T is larger than 325 K. In order to

obtain accurate data of atomic density as the function of the temperature, the absorption rate should be measured to correct the intensity data of F_m.

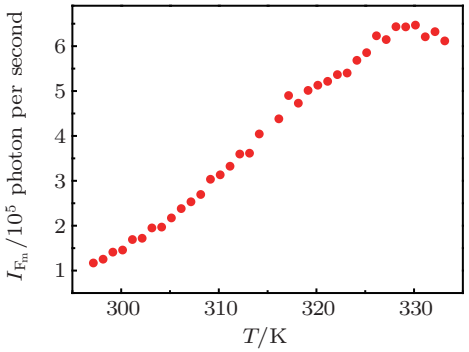


Fig. 2. (color online) Measured intensity of fluorescence F_m as the function of the temperature of the cell C.

We use another laser beam R with horizontal polarization to simulate fluorescence F_m. The experimental setup is shown in Fig. 3, almost the same as that in Fig. 1(c), except the beam R. The beam R comes from another external-cavity diode laser, whose frequency is the same as that of F_m, and is split into two beams ($R_{1,2}$) before entering the cell C. The intensities of R_1 and R_2 are identical and can be changed by rotating the half waveplate HWP. The R_1 beam, spatially overlapping with F, is used to simulate the absorption of F_m. The intensity of R_1 beam after the etalon is controlled to be equal to that of F_m at different temperatures. The R_2 beam is detected directly by single photon detector D_2 (PerkinElmer, SPCM-AQRH-14-FC) as the intensity reference of R_1. Dividing the intensity of R_1 by that of R_2, we can obtain the transmission rate of the R_1 photon ($\eta_{\text{Tran}-R_1}$) with horizontal polarization.

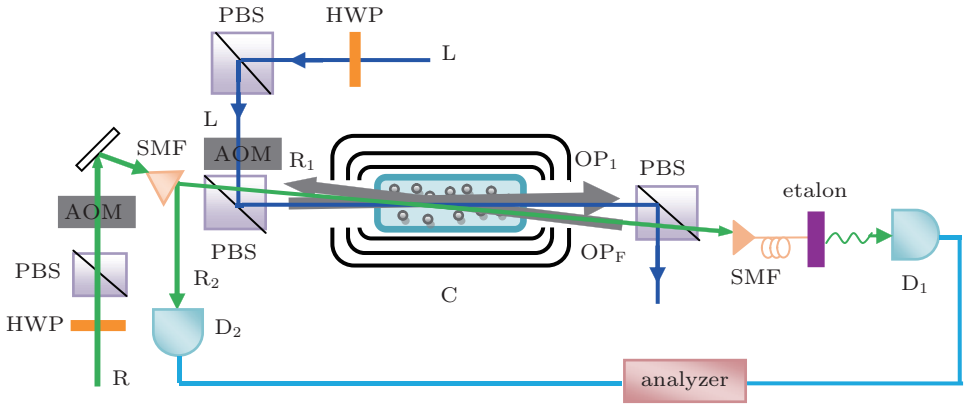


Fig. 3. (color online) Experimental setup for absorption compensation. The diameter of R_1 is the same as the detected fluorescence F. When we measure the intensity of F_m, the beam R is blocked. When the intensities of R_1 and R_2 are measured, the beam L is blocked.

The measured transmission rate of the R_1 photon ($\eta_{\text{Tran}-R_1}$) as the function of the cell temperature is shown in Fig. 4(a) (square curve). In general, the transmission rate is larger at lower temperature than that at higher temperature because of the absorption, as analyzed above. Another notable character is the typical oscillation with the temperature, which is due to the optical rotation. In experiment, the R_1 beam is linearly polarized and far off-resonant on the transition from $|g\rangle$ to $|e_1\rangle$. Meanwhile, the atomic vapor is spin polarized (most atoms populate at the $|g\rangle$ level). According to the theory of the optical rotation, when linearly polarized laser transmits through the spin-polarized atomic vapor, its plane of polarization will rotate by an angle θ due to the difference in the refraction indices $n_+(v)$ and $n_-(v)$, which are experienced by σ^+ and σ^- lights, respectively. After traveling through the atomic vapor with the length l, the rotated angle θ of the polarization can be written as[20]

$$\theta = \pi l\,[n_+(v) - n_-(v)]\,/\lambda, \tag{1}$$

$$[n_+(v) - n_-(v)] \propto N, \tag{2}$$

where λ is the wavelength of the laser, and N is the atomic number in the vapor. In our experiment, the length l and wavelength λ are fixed, so finally

$$\theta \propto N. \tag{3}$$

The rotated angle of the R_1 polarization is proportional to the atomic number. This is the reason why the R_1 intensity after the PBS shows oscillation behavior. Thus, the transmission rate of the R_1 beam ($\eta_{\text{Tran}-R_1}$) after the PBS should be written as

$$\eta_{\text{Tran}-R_1} = \eta_{\text{Tran}-\text{Abs}} \times \eta_{\text{Tran}-\text{Rot}}, \tag{4}$$

where $\eta_{\text{Tran}-\text{Abs}}$ is the transmission rate related to the absorption by the $|m\rangle$ atoms, $\eta_{\text{Tran}-\text{Rot}}$ is the transmission rate related to the rotation effect of the linear polarization. In case of the fluorescence F_m, its polarization is random, so the rotation effect on F_m can be neglected. That is to say, $\eta_{\text{Tran}-\text{Rot}} \sim 1$. The transmission rate of F_m ($\eta_{\text{Tran}-F_m}$) should be equal to the value of $\eta_{\text{Tran}-\text{Abs}} = \eta_{\text{Tran}-R_1}/\eta_{\text{Tran}-\text{Rot}}$. The intensity of the F_m photon in Fig. 2 can be corrected by dividing the factor $\eta_{\text{Tran}-\text{Abs}}$.

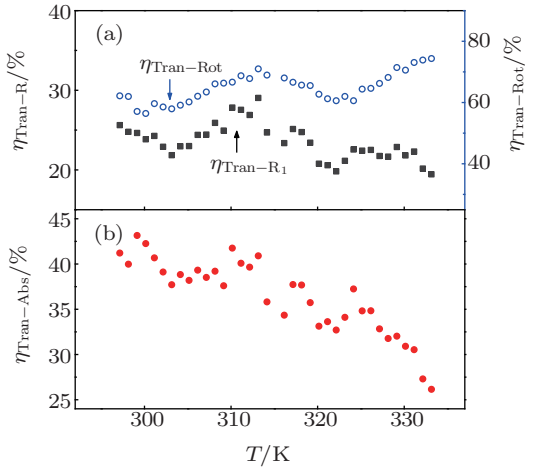


Fig. 4. (color online) (a) Black square: the transmission efficiency of the R_1 photon; blue circle: the transmission rate of the R_1 photon caused by the polarization rotation effect. (b) Transmission rate of the R_1 photon caused by the absorption effect.

The optical rotation is measured by blocking the laser L in Fig. 3, and the result is given in Fig. 4(a) (circle curve). The frequency of R_1 laser is blue detuning 1.5 GHz from the transition $|m\rangle \rightarrow |e_1\rangle$ to remove the absorption effect. The oscillation in the square curve is similar to that in circle curve. The $\eta_{\mathrm{Tran-Abs}}$ value is calculated and given in Fig. 4(b). The final intensity of F_m photon is corrected and shown in Fig. 5, where its intensity increases with the temperature monotonically.

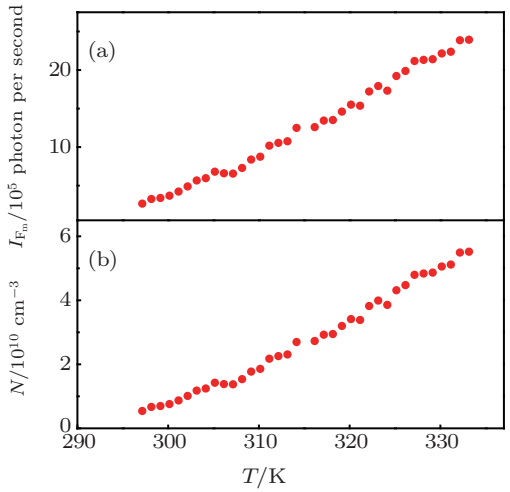


Fig. 5. (color online) (a) The final intensity of fluorescence F_m as a function of temperature after absorption compensation. (b) The atomic density of ^{87}Rb as the function of temperature.

4. Experimental fitting function

The saturation intensity of the ^{87}Rb D_1 line is[21] 4.4876(31) mW/cm^2. In our experiment, the intensity of the laser L is smaller than the saturation intensity, so the absorption of the laser L follows Beer–Lambert's law

$$I = I_0\,\mathrm{e}^{-k_0 l}, \tag{5}$$

where I_0 and I are the intensity before and after the vapor, respectively; l is the distance that the laser travels through the vapor; and, k_0 is the absorption coefficient and can be written as[22]

$$k_0 = \frac{2}{\Delta\nu_{\mathrm{D}}}\frac{{\lambda_0}^2 g_2}{8\pi g_1}\frac{N}{\tau}, \tag{6}$$

where λ_0 is the wavelength, g_1 and g_2 are the statistical weights of the lower and upper states, $\Delta\nu_{\mathrm{D}}$ is the Doppler width of the absorption line, N is the density number of the vapor, and τ is the lifetime of the upper state. Then the fluorescence intensity I_{f} can be written as

$$I_{\mathrm{f}} = I_0(1-\mathrm{e}^{-k_0 l})\phi, \tag{7}$$

where ϕ is the fluorescence quantum efficiency. Thus, the atomic density can be written as

$$N = -\frac{\Delta\nu_{\mathrm{D}}}{2}\frac{8\pi g_1}{{\lambda_0}^2 g_2}\frac{\tau}{l}\ln\left(1-\frac{I_{\mathrm{f}}}{I_0\phi}\right). \tag{8}$$

Finally, the experimental atomic density of the ^{87}Rb vapor is shown in Fig. 5(b).

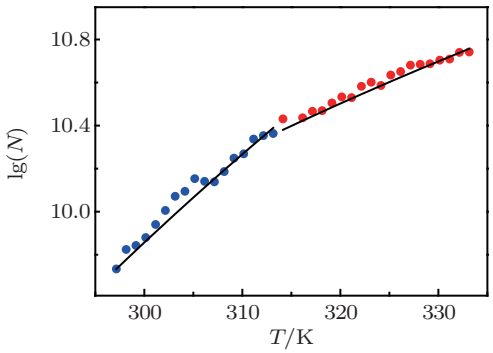


Fig. 6. (color online) Plot of $\lg(N)$ versus temperature. Square: experimental data. Solid lines: fitting results.

In general, the functions of the atomic density N and vapor pressure p are usually reported in terms of[15]

$$\lg(N) = -A/T-(B+1)\lg(T)+C+DT+18.985, \tag{9}$$

$$\lg(p) = -A/T-B\lg(T)+C+DT, \tag{10}$$

where the unit of N is cm^{-3}, p is in torr, and T is in kelvin. The melting point of ^{87}Rb is 312.31 K, we fit the experimental data in Fig. 6 with Eq. (9) in two temperature ranges, corresponding to solid phase (297–312.31 K) and liquid phase (312.31–334 K). The fitting results are

$$\begin{aligned}\lg(N) \;=\; & -2006.26/T+39.075\lg(T)\\ & -3.622\times10^{-2}T-69.38326\end{aligned} \tag{11}$$

for 297–312.31 K,

$$\begin{aligned}\lg(N) \;=\; & -3200.557/T-8.466\lg(T)\\ & +5.8\times10^{-3}T+41.527\end{aligned}$$

for 312.31–334 K.

5. Conclusion

We experimentally measured the atomic density of the ^{87}Rb vapor in the range of 297–334 K mainly using fluorescence measurement. The data accuracy was ensured by combination of several approaches including the lasers with narrow bandwidth, the cell with anti-reflection coating (paraffin coating), optical pumping, single-photon detection system, and absorption compensation. The fluorescence method is a sensitive way to measure vapor density. In previous experiments,[14–17] the main error came from depopulation of the energy level, self-absorption, and broad bandwidth of the laser. In our experiment, the bandwidth of the laser L (300 kHz) is much smaller than the width of Doppler broadening of the ^{87}Rb vapor, so the inaccuracy from the broad-bandwidth effect was eliminated. The strong OP laser prepared most atoms populated on the $|g\rangle$ level before the fluorescence measurement, so the self-absorption effect, resulting from the absorption of F_m by the $|m\rangle$ atoms, was greatly weakened. The coherent time of the atoms in the paraffin-coated cell (100 milliseconds) is much longer than that in a normal cell, and the depopulation effect was reduced. The single-photon detection system, especially with three kinds of filters, was used to decrease the noise from the leaking L and OP lasers in fluorescence measurement. The self-absorption from rest $|m\rangle$ atoms was calibrated by the absorption compensation. Finally, there are some residual ^{85}Rb atoms in the ^{87}Rb vapor, which contributed about 3%–5% error to the data of atomic density.

References

[1] Marte A, Volz T, Schuster J, Dürr S, Rempe G, van Kempen E G M and Verhaar B J 2002 *Phys. Rev. Lett.* **89** 283202
[2] Zhou Z C, Wei R, Shi C Y, Li T and Wang Y Z 2011 *Chin. Phys. B* **20** 034206
[3] Qu S P, Zhang Y and Gu S H 2013 *Chin. Phys. B* **22** 099501
[4] Hosseini M, Sparkes B M, Campbell G, Lam P K and Buchler B C 2011 *Nat. Commun.* **2** 174
[5] Vudyasetu P K, Starling D J and Howell J C 2009 *Phys. Rev. Lett.* **102** 123602
[6] Su J, Deng K, Guo D Z, Wang Z, Chen J, Zhang G M and Chen X Z 2010 *Chin. Phys. B* **19** 110701
[7] Zhou H T, Wang D, Guo M J, Gao J R and Zhang J X 2014 *Chin. Phys. B* **23** 093204
[8] Yoshikawa Y, Torii Y and Kuga T 2005 *Phys. Rev. Lett.* **94** 083602
[9] Sheng D, Li S, Dural N and Romalis M V 2013 *Phys. Rev. Lett.* **110** 160802
[10] Liu G B, Sun X P, Gu S H, Feng J W and Zhou X 2012 *Physics* **41** 803
[11] Vanier J 2005 *Appl. Phys. B* **81** 421
[12] Li S L, Xu J, Zhang Z Q, Zhao L B, Long L and Wu Y M 2014 *Chin. Phys. B* **23** 074302
[13] Chen S, Chen Y A, Strassel T, Yuan Z S, Zhao B, Schmiedmayer J and Pan J W 2006 *Phys. Rev. Lett.* **97** 173004
[14] Killian T J 1926 *Phys. Rev.* **27** 578
[15] Gallagher A and Lewist E L 1973 *J. Opt. Soc. Am.* **63** 864
[16] Fairbank W M, Jr Hänsch T W and Schawlow A L 1975 *J. Opt. Soc. Am.* **65** 199
[17] van der Spek A M, Mulders J J L and Steenhuysen L W G 1988 *J. Opt. Soc. Am. B* **5** 1478
[18] Tehranchi M M, Hamidi S M and Abaie B 2013 *Journal of the Korean Physical Society* **62** 731
[19] Olson A J and Mayer S K 2009 *Am. J. Phys.* **77** 116
[20] Seltzer S J 2008 *Developments in Alkali-Metal Atomic Magnetometry* pp. 32–37 (America: Princeton University)
[21] Steck D A *Rubidium* 87 *D Line Data* (Los Alamos National Laboratory)
[22] A Product Of Teachspin 2002 *Optical Pumping of Rubidium* (New York)